

CASE STUDY ANALYSIS OF A PELAMIS WAVE-ENERGY CONVERTER

Enrique L. P. Statquevios, Guilherme Marchioro, Pedro V. H. V. Garcia, Paulo F. Lamarão, Walter J. P. Casas

*Department of Mechanical Engineering, Federal University of Rio Grande do Sul
Rua Sarmiento Leite 435, 90050-170, Porto Alegre/Rio Grande do Sul, Brasil
eleonps@gmail.com, gui02_marchioro@hotmail.com, pedrovictor86@gmail.com,
paulo.fuza.lamarao@gmail.com, walter.paucar.casas@ufrgs.br*

Abstract. Having in mind the objectives defined by the UN 2030 agenda, researches such as those resulting from the ondomotriz principle grew in importance. Therefore, this work aims to evaluate the potential energy conversion provided by a Pelamis device in a study case for Rio Grande - RS. The development of the research is made through parameterized numerical simulations, which were performed using ANSYS AQWA software. Specific issues were necessary about verification of mesh refining convergence, time step definition and application of monochrome waves belonging to the study area sea state. Relative to the anchorage system, the catenaries composition was determined through an iterative routine using the MATLAB software. The simulations returned data about the movement of the cylinders, which were processed in MATLAB aiming to quantify, plot and evaluate the rotation in the joint between the cylinders. Thus, the stability of the mechanism and the possible power generation potential is evaluated. The study demonstrates an important relationship between the structure length and the wavelength. Finally, from the analysis of the results, the study suggests the best parameters combination for the researched location.

Keywords: Pelamis sizing, wave energy, numerical simulation, energy conversion, stability analysis.

1 Introduction

In 2015, the United Nations (UN) released the 2030 agenda for sustainable development, a document which enumerates 17 development goals to be achieved for a better world. Attempting to the objectives related to “Affordable and Clean Energy” and “Industry, Innovation and Infrastructure”, renewable energy generation devices becomes more relevant.

With that in mind, it is verified that the energetic potential of the sea can reach up to 2 TW (Thorpe [1]) and the marine converters generate energy about 90% of the operating time (Pelc and Fujita [2]). Thereby, it can be emphasized the Pelamis marine energy converter (Fig. 1a), both for its ease of installation and the use of its own buoyancy as a source of reaction force (Eden [3]). Among the works involving this type of converter, the research made by Alves [4] seeks to size the mechanism based on the interest site; the work of Hongzhou *et al.* [5] evaluates the angular movement between the cylinders and the work of Eden [3] aims to evaluate the energy absorption efficiency of the Pelamis.

Therefore, it is important to pay attention to all aspects mentioned above to evaluate the Pelamis behavior. This work aims to size 3 different Pelamis structures, based on the most frequent sea waves of Rio Grande-RS, Brazil, and perform hydrodynamic simulations of the structures excited by these waves using ANSYS AQWA, in order to assess the mechanism stability and the angular movement between the cylinders. Thereby, it is possible to evaluate the energy conversion potential of the device and suggest the best Pelamis module length range for the application site.

2 Wave definitions

In order to define the wave characteristics of the study area, data from the Brazilian Coast Monitoring System (SiMCosta) was used, obtained via an acquisition buoy located above 13 m depth, in front of Casino beach, Rio Grande-RS, Brazil (SIMCOSTA [6]).

The average height and period data were obtained from the website, gathering information from February 2019 to April 2020. The data in the form of temporal series were treated separately, fitted with normal distributions aiming to restrict the values to a highest occurrence range, in order to select the information that better represents the sea state. The height and period were restricted to a 60% range of occurrence around the average, attempting to the limits where it occurs. In addition to these limits, two intermediate values of periods were used, on a range of 20% of occurrence. Also, the average height was used.

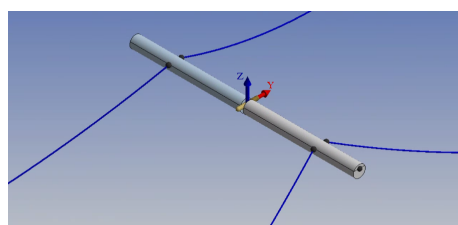
The waves used on the simulations, resulting from the combination of the previously discussed data, are shown in Table 1, which describes the periods, heights and wavelengths (L).

Table 1. Sea state

Wave	Height (m)	Period (s)	L (m)	Wave	Height (m)	Period (s)	L (m)	Wave	Height (m)	Period (s)	L (m)
1	0.4806	4.2294	27.8481	5	0.7214	4.2294	27.8481	9	0.9622	4.2294	27.8481
2	0.4806	4.8886	36.8475	6	0.7214	4.8886	36.8475	10	0.9622	4.8886	36.8475
3	0.4806	5.4554	45.1054	7	0.7214	5.4554	45.1054	11	0.9622	5.4554	45.1054
4	0.4806	6.1144	54.9187	8	0.7214	6.1144	54.9187	12	0.9622	6.1144	54.9187



(a)



(b)

Figure 1. Pelamis example: (a) in operation (YEMM et. al. [7]) and (b) simulation model

3 Sizing

In the same way as the wave definitions, the structure sizing in terms of length, diameter and spacing between the modules was designed based on the average of wavelengths and the limits which 60% of them occur. Working toward a maximum energy absorption, the module length was calculated, as recommended in Alves [4], as being the half of the wavelength. The diameter (d) was calculated according to an average ratio between the length (C) and the diameter of each module (C/d) of different Pelamis studied by several authors. This average ratio result in a value of 9.57, and the source studies are shown in Table 2. Lastly, the minimum spacing (e_{min}) between the two modules was calculated ensuring no collision on a critical wave, which has the highest wave height registered among those acquired and a 60% bottom limit period, since this would generate the greatest angle (θ_{max}) between the Pelamis module and the waterline. The idea of the calculation is presented in Fig. 2, which demonstrates the relationship between the minimum acceptable spacing and the maximum angle generated by the critical wave.

Table 2. Parameters given by other studies and used for the diameter calculation

Parameter	Alves [4]	Yemm et al. [7]	Cruz and Sarmiento [8]	Mahmoodian et al. [9]	Karim et al. [10]
Length	30	36	30	35	36
Diameter	3	4	3.5	3.5	3.5
Quantity	2	5	4	4	5
C/d	10	9	8.57	10	10.28

The proposed geometries are presented in Table 3, which were rounded in this work. The spacing (e) between the modules, in view of being a critical part of the project, was also rounded upwards for safety.

Since Pelamis is an offshore structure and aiming to restrict the translation and stabilize the structure, a catenary anchorage configuration was chosen in accordance to Fitzgerald and Bergdahl [11]. A routine in MATLAB

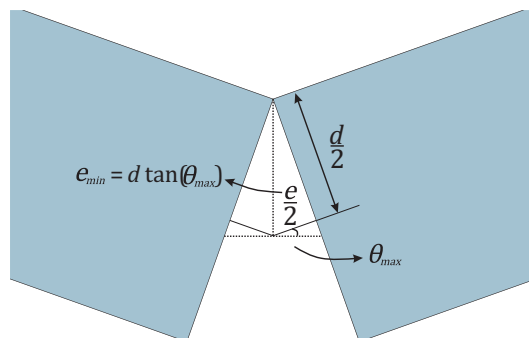


Figure 2. Idea used to calculate the spacing

was made to calculate the required parameters to obtain a consistent catenary. Employing Faltinsen [12] equations, the cable is sized to support all the forces caused by the structure. Also, the routine takes into account material properties with information obtained from the Bridon manufacturer catalog (BRIDON [13]). The material chosen was a polyester cable which has a weight per meter in air equal to 10 kg/m and maximum tension of 3924000 N. Table 4 shows the final anchoring dimensions, where l_t stands for total length, l_s the suspended length, p_f is the fixed point, θ_a is the angle between the waterline and the catenary, and δ_m the maximum horizontal variation of movement. Figure 1b illustrates the model arrangement used in the simulations, in which there are two catenary cables connected to each module and, at the center, connecting the cylinders, a joint that allows rotation only in one axis.

Table 3. Proposed structures

Pelamis	Length	Diameter	Spacing
1	14 m	1.5 m	0.4 m
2	20 m	2.0 m	0.5 m
3	27 m	3.0 m	0.7 m

Table 4. Anchorage properties

	l_t (m)	l_s (m)	p_f (m)	θ_a (°)	δ_m (m)
Pelamis 1	253.34	146.65	252.67	10.13	0.32
Pelamis 2	213.01	123.44	212.10	12.02	0.39
Pelamis 3	95.97	56.42	93.95	25.95	0.84

4 Numerical modeling

The dynamic behavior of the floating structure is numerically modeled based on a mass-spring-damper system composed by six degrees of freedom, as described in Chakrabarti [14], shown in equation:

$$\mathbf{M}_T \ddot{\mathbf{x}}(t) + \mathbf{C} \dot{\mathbf{x}}(t) + \mathbf{K} \mathbf{x}(t) = \mathbf{F}_{ext}(t), \quad (1)$$

which \mathbf{M}_T is the sum of the structural and additional mass, \mathbf{C} is the viscous damping and \mathbf{K} is the cable stiffness added with the stiffness due to the structure restoring part. All these components being matrices. The vectors $\ddot{\mathbf{x}}$, $\dot{\mathbf{x}}$ and \mathbf{x} denote the acceleration, velocity and displacement, respectively.

The excitation forces are expressed by the vector \mathbf{F}_{ext} , which are described by the next equation, where $\mathbf{F}_{fk}(t)$ is the Froude-Krylov force and $\mathbf{F}_{dif}(t)$ is the diffraction force:

$$F_{ext}(t) = F_{fk}(t) + F_{dif}(t). \tag{2}$$

Froude-Krylov force, described in eq. (3) and eq. (4), is exerted in the structure by the pressure field generated by waves not disturbed due to the structure presence. According to Chakrabarti [14], it is determined by the integral of the dynamic pressure (p_d) with respect to the submerged surface:

$$F_{fkx} = C_H \iint_S p_d n_x dS, \tag{3}$$

$$F_{fkz} = C_V \iint_S p_d n_z dS. \tag{4}$$

C_H and C_V are force coefficients related to horizontal and vertical directions, n_x and n_z are the normal directions of horizontal and vertical axis, respectively. Based on the linear wave theory, the pressure gradient from a wave passage is represented by eq. (5) (Dean and Darlymple [15]):

$$p(x, z, t) = \rho g \frac{H}{2} \frac{\cosh(k(h+z))}{\cosh(kh)} \cos(kx - \omega t) - \rho g z. \tag{5}$$

With ρ being the water density, g the gravitational acceleration, H the wave height and $k = 2\pi/L$ the wave number. The depth is expressed by h and ω is the wave angular velocity.

The force excitation due to diffraction is also obtained from the pressure integral along the body structure, however with boundary conditions associated to dynamic pressure modifications forced by the structure presence. Therefore, its simplification to a first-order system according to Chakrabarti [14] is given by:

$$F_{dif} = \varepsilon \iint_S p_1 n dS. \tag{6}$$

ε is the perturbation parameter and p_1 is the first-order portion of the pressure derived from the Laplace equation solving due to a potential flow, limited to certain boundary conditions.

To solve those equations, the ANSYS AQWA software splits the structure in discrete parts, in a process known as the panel method, allowing the evaluation of the potential flow around the body, and then applies the necessary boundary conditions to solve the differential equations.

5 Mesh refinement and timestep

A mesh refinement verification process is required, and the best way to do it, according to Massie [16], is by performing simulations and checking the convergence of results.

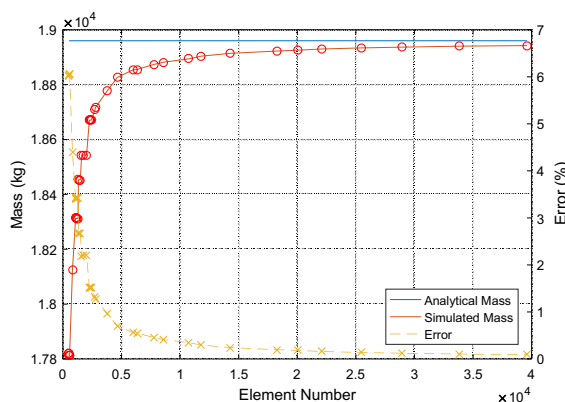


Figure 3. Mesh refinement convergence of 14 m length Pelamis

Defining that, in hydrostatic equilibrium, the modules would have 70% of the diameter submerged in water, the analytical mass was calculated. After that, it was compared with the numerical mass obtained by ANSYS for the same hydrostatic condition. Starting from a mesh with few elements, which were progressively being increased, it was possible to notice the convergence of values. At the end, meshes with approximately 10,000 elements were chosen in the 3 cases, resulting in an error close to 0.35% between the software calculation and the analytical mass. Figure 3 shows the iterative process of refinement to the Pelamis type 1 .

The time step selection was based on the recommendation of the ANSYS manual [17], which states that the maximum value must be less than one tenth of the shortest wave period for the simulation convergence. Thus, starting from the value of 0.42 s, progressively smaller time steps were tested until a response convergence was found for a value of 0.1 s.

6 Results and discussion

After simulating all the Pelamis described in Table 3 for each wave presented in Table 1, graphs were plotted aiming to quantify the relative angular displacements between the modules, which are defined by:

$$\theta_{rel} = 180^\circ - (\theta_{pos} + \theta_{neg}). \tag{7}$$

Being θ_{pos} and θ_{neg} the longitudinal axis angles of the two cylinders with respect to the waterline. The angular displacement was obtained in order to evaluate the stability of the converter related to the wave and its length, in addition to evaluating the energy potential.

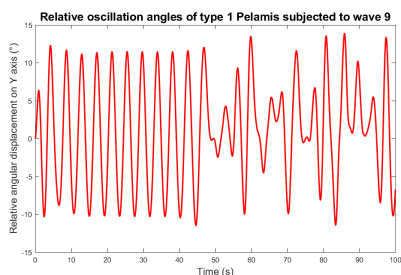
Analyzing the angle-time graphs, it is possible to notice a sinusoidal behavior in all cases, except in the simulation corresponding to wave 9 (height 0.9622 m and period 4.2294 s) submitted to Pelamis 1. The graph for this case is shown in Fig. 4a, which can be compared with other responses from different situations that have more uniform graph formats, as shown in Fig. 4b, Fig. 4c and Fig. 4d.

Attesting the difference in behavior between the conditions of Fig. 4a and the others, Fig. 4b and Fig. 4c also refer to wave 9, but concerning to Pelamis of type 2 and 3 respectively, which demonstrates sinusoidal behavior. Figure 4d shows the sinusoidal behavior of the relative angular displacement response of Pelamis type 1 to wave 10, envincing that, even when both structures are the type 1 Pelamis, they do not respond equally to the waves.

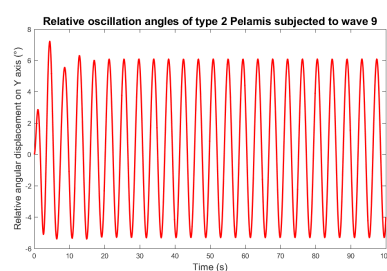
Additionally, by plotting the Pelamis 1 response when exposed to wave 9 combined with its wave slope angle, both varying with respect to the simulation time, it is confirmed that the irregular waveform obtained is resultant from a device instability (Fig. 5). The instability of Pelamis 1 in wave 9 suggests that the ratio between maximum wave steepness and Pelamis length is the limit value for stability, however, a deeper analysis is needed to verify this correlation.

In order to quantify the energy potential, the RMS values of the relative angles between the modules were calculated and the results are shown in Table 5. The gradient in Table 5 varies from green to red, as the angle decreases. The wave column refers to the waves defined in Table 1.

Attempting to the wavelength of waves 1, 5 and 9, available in Table 1, it is noticed that its value is approximately 28 m, being twice the length of the Pelamis 1, which, precisely for these waves, presents greater oscillation when compared to other waves of the same height. Similarly, it is verified that waves with wavelengths closer to twice the length of the 20 m and 27 m Pelamis are the ones with the greatest oscillation in these devices. In addition, analyzing Table 1 together with Table 5, it is noticed that the higher the wave height, the greater the RMS value of the relative angle between the modules.



(a) Pelamis 1 exposed to wave 9



(b) Pelamis 2 exposed to wave 9

Another analysis is done with the simulation results, aimed to find out which of the 3 Pelamis oscillates the most combining the results of the 12 simulated waves. This data is presented in Table 6 below, which contains the average of the RMS angular displacements between the 12 input waves for each device.

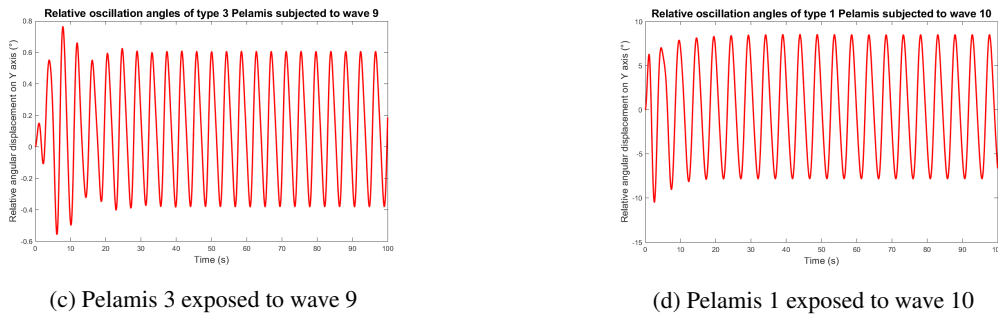


Figure 4. Relative angular displacement between cylinders of different lengths exposed to different waves

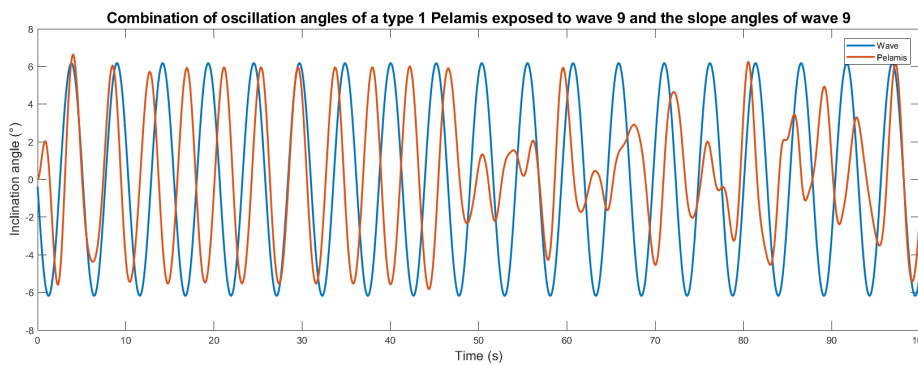


Figure 5. Combination of oscillation angles of a type 1 Pelamis exposed to wave 9 and the slope angles of wave 9

Angular displacement is the main variable that implies the power generation potential of the Pelamis-type converter, but in addition to it, it is also important to pay attention at the moment generated by each module, since the moment arm varies according to the length and diameter of the device.

Table 5. RMS values of the relative angle between the modules

Wave	Pelamis length (m)			Wave	Pelamis length (m)			Wave	Pelamis length (m)		
	14	20	27		14	20	27		14	20	27
1	3.7719	2.0753	0.2373	5	5.6618	3.0337	0.2895	9	6.7913	4.0334	0.3589
2	2.8366	2.7072	1.4253	6	4.2477	3.9847	2.1340	10	5.6563	5.2809	2.9571
3	2.1889	2.4616	1.9602	7	3.2724	3.6467	2.9177	11	4.3534	4.8126	4.1015
4	1.6487	1.9843	1.9679	8	2.4602	2.9496	2.9224	12	3.3132	3.9252	3.891

Table 6. Average RMS values of the relative angle between the modules

Pelamis length (m)	14	20	27
Average RMS angle (°)	3.8502	3.4079	2.0968

7 Conclusion

By analyzing the RMS relative angular displacement data from the simulations and considering the characteristic length of each wave, it is possible to verify the proposed correlation between incident wavelength and the length of the Pelamis cylinder.

It was noticed that the converter that presented the greatest energy potential was the one that also presented instabilities, demonstrating that it is necessary to balance these two parameters in order to propose a Pelamis that

works fine for the interest location. Therefore, it is concluded that a Pelamis with a length much less than half the wavelength of the interest place sea state does not work properly, as it tends to become unstable since the ratio of steepness to Pelamis length can exceed the simulated limit value. In addition, for larger Pelamis lengths, when compared to the wavelength, it is verified some difficulty in obtaining large relative angular displacements between the modules, which implies low potential energy generation.

Thus, for Rio Grande-RS, Brazil, in view of the presented results, it is indicated a Pelamis converter device with lengths in a range of 14 to 20 m in order to provide greater capacity for energy conversion from the most frequent waves evaluated by the study. Due to the joint model used for the two cylinders, the results obtained with this work are applicable for a Pelamis that has a power generation system with minimum stiffness and damping, parameters reflected in the used joint. To verify the influence of the moment generated by the modules, simulations with more resistant joints would have to be carried out, which would translate into more rigid energy generation systems, thereby possibly modifying the structure's response and consequently the angular displacement.

Acknowledgements. This study was financed in part by the Coordination for the Improvement of Higher Education Personnel – Brasil (CAPES) – Finance Code 001, the National Council for Scientific and Technological Development (CNPq) and Rio Grande do Sul State Research Support Foundation (FAPERGS).

Authorship statement. The authors hereby confirm that they are the sole liable persons responsible for the authorship of this work, and that all material that has been herein included as part of the present paper is either the property (and authorship) of the authors, or has the permission of the owners to be included here.

References

- [1] Thorpe, T. W., 1999. *A brief review of wave energy*. UK Department of Trade and Industry.
- [2] Pelc, R. & Fujita, R.M., 2002. *Renewable energy from the ocean*. Marine Policy, pp.475.
- [3] Eden, J. A., 2013. *Optimum design of the pelamis wave energy converter*. MSc dissertation. California State University, Sacramento.
- [4] Alves, V. W., 2009. *Dimensionamento e resposta dinâmica de um gerador de energia das ondas*. Trabalho de Conclusão do Curso de Engenharia Mecânica. UFRGS, Escola de Engenharia.
- [5] Hongzhou, H. & Quanyou, Q. & Juyue, L., 2013. Numerical simulation of section systems in the pelamis wave energy converter. *Advances in Mechanical Engineering*, vol. 2013, pp.1-8.
- [6] SIMCOSTA. *SiMCosta Portal*, 2020. Available: <http://www.simcosta.furg.br/home>. Access in April, 2020.
- [7] Yemm, R. & Pizer, D. & Retzler, C. & Henderson, R., 2011. *Pelamis: experience from concept to connection*. Philosophical Transactions of The Royal Society A (2012) 370, pp. 365-380.
- [8] Cruz, J. M. B P. & Sarmiento, A. J. N. A., 2004. *Energia das Ondas: Introdução aos Aspectos Tecnológicos, Econômicos e Ambientais*. WEC – Wave Energy Centre.
- [9] Mahmoodian, M., 2009. *Impact assesment of a new wave energy converter, Anaconda*. MSc Dissertation. University of Southampton.
- [10] Karim, M. A. & Noor, Md. H. & Nasim, M. & Khan, S. I., 2015. Assesment of a simplified model of a wave energy converter in terms of hydraulic mechanical and electrical parameters. *International Journal of Energy and Power Engineering*, volume 4, Issue 2, April 2015, Pages: 94-102.
- [11] Fitzgerald, J., & Bergdahl, L., 2007. Including moorings in the assessment of a generic offshore wave energy converter: A frequency domain approach. *Marine Structures*, vol. 21, pp. 23-46.
- [12] Faltinsen, O. M., 1990. *Sea loads on ships and offshore structures*. Cambridge University Press.
- [13] BRIDON. Bridon Oil and Gas. 2013. *Products Catalogue*. Doncaster, UK.
- [14] Chakrabarti, S. K., 1987. *Hydrodynamics of offshore structures*. WIT press, London, UK.
- [15] Dean, R. G. & Dalrymple, R. A., 1991. *Water wave mechanics for engineers and scientists*. World Scientific, Singapore.
- [16] Massie, W. W., 2001. *Offshore hydromechanics*. Delft University of Technology.
- [17] ANSYS. 2016. *ANSYS Manual. Release 16.0*.